ACS APPLIED MATERIALS & INTERFACES

RESEARCH ARTICLE

www.acsami.org

Control of Microfluidic Flow in Amphiphilic Fabrics

Tracie L. Owens,[†] Johannes Leisen,[§] Haskell W. Beckham,[‡] and Victor Breedveld*[,†]

[†]School of Chemical and Biomolecular Engineering, [§]School of Chemistry and Biochemistry, and [‡]School of Materials Science and Engineering, Georgia Institute of Technology, Atlanta, Georgia 30332, United States

ABSTRACT: Woven textile fabrics were designed and constructed from hydrophilic and hydrophobic spun yarns to give planar substrates containing amphiphilic microchannels with defined orientations and locations. Polypropylene fibers were spun to give hydrophobic yarns, and the hydrophilic yarns were spun from a poly(ethylene terephthalate) copolyester. Water wicking rates into the fabrics were measured by video microscopy from single drops, relevant for point-of-care microfluidic diagnostic devices, and from reservoirs. intra-yarn microchannels in the hydrophilic polyester yarns were shown to selectively transport aqueous fluids, with the flow path governed by the placement of the hydrophilic yarns in the fabric. By comparing fluid transport in fabric constructions with systematic variations in the numbers of adjacent parallel and orthogonal hydrophilic yarns, it was found that inter-yarn microchannels significantly increased wicking rates. Simultaneous wicking of an aqueous and hydrocarbon fluid into the hydrophilic and hydrophobic microchannels of an amphiphilic fabric was successfully demonstrated. The high degree of interfacial contact and micrometer-scale diffusion lengths of such coflowing immiscible fluid streams inside amphiphilic fabrics suggest potential applications as highly scalable and affordable microcontactors for liquid−liquid extractions.

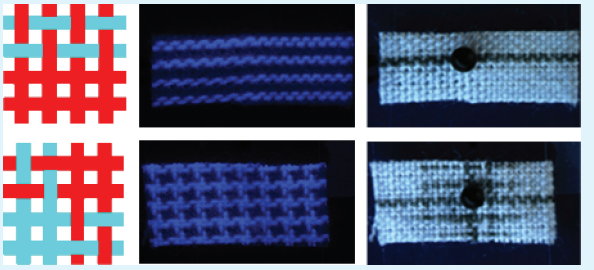

KEYWORDS: microfluidic, fabric, thread, liquid−liquid extraction, wicking

INTRODUCTION

In this study, fabrics were systematically engineered to exhibit amphiphilic properties to achieve microfluidic coflow of immiscible liquid phases within the void spaces. The fabrics show potential for use as media for large-scale chemical processing applications, in particular liquid−liquid extractions with reduced waste volumes and increased efficiency. The novel amphiphilic substrates can also provide inexpensive, high-volume production alternatives for microfluidic device fabrication.

The research described in this paper was inspired by work in microfluidics, the field of research and engineering that studies geometrically constrained fluids within micrometer-sized structures, usually in the form of intricate networks of interconnected channels and reservoirs on small "microfluidic chips".[1,2] The small dimensions of microfluidic channels result in large surface-area-to-volume ratios, strong wall−fluid interactions, and dominance of diffusive processes in fluidic transport.[2] As a consequence, manipulation of physical and chemical properties of the channels (e.g., shape, connectivity, surface energy, and wettability of walls) enables precise control over fluid flow. Microfluidic chips can thus be engineered to transport small volumes of fluids to precise locations on the chip, where (bio)chemical reactions can be carried out. This concept has proven particularly beneficial in biomedical applications, such as rapid analysis of patient biofluids for disease detection or drug screening, and in fundamental biological and chemical studies.[1,3]

Although alternative methods exist, soft lithography is currently the predominant technology for manufacturing microfluidic devices: complex 2D and 3D channel structures are created in a polydimethylsiloxane (PDMS) elastomer mold,[2] which is typically bonded to a glass or silicon substrate for mechanical support.[1] The high degree of fluid flow control offered by these devices is appealing for many application areas, but the soft-lithography manufacturing process limits commercially viable use to specialized high-value applications with small volumetric throughput of liquids, mostly in the biomedical area. Recent advances toward cheaper microfluidic devices have largely been driven by the desire to deploy point-of-care (POC) diagnostic screening kits in developing countries for detection of common diseases.[1] These efforts have focused on replacement of PDMS with alternative substrate materials. Cheap, porous materials that can efficiently wick liquids via capillary action, like paper and cotton yarns, have emerged as primary candidates, because capillary flow eliminates the need for external power sources to generate flow.[1] Paper, however, wicks fluid isotropically; control over the rate and direction of liquid flow within this substrate requires the use of hydrophobic barrier materials (e.g., SU-8 photoresist or wax-like ink)[4−6] to create flow channels inside the hydrophilic paper, or careful design of the shape of the paper substrate.[7,8] Capitalizing on the inherent directionality of the voids in cotton yarns, other researchers have integrated yarns (i.e., threads) as fluid channels into polymer substrates to create low-cost microfluidic devices for medical diagnostics.[9−11] Additionally, the use of threads with different wettability (i.e., hydrophobic and hydrophilic yarns) in polymer substrates has been employed as a method to manipulate liquid transport and stimulate mixing of phases.[10]

Received: July 29, 2011
Accepted: September 26, 2011
Published: September 26, 2011

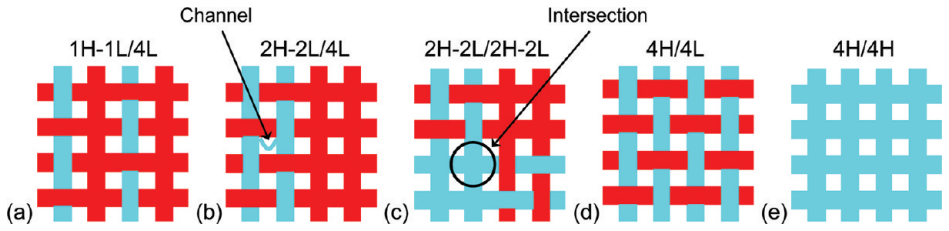

Figure 1. Schematics of five fabric samples examined in this study. The red (dark) yarns represent hydrophobic (or lipophilic) yarns (L), whereas the blue (light) yarns represent hydrophilic yarns (H): (a)1H-1L/4L, (b)2H-2L/4L, (c)2H-2L/2H-2L, (d)4H/4L, (e)4H/4H (purely hydrophilic control fabric). Highlighted are examples of a "channel" and an "intersection", key structural features of the amphiphilic fabrics with regards to fluid transport.

Paper- and yarn-based microfluidic structures not only offer more scalable production methods for microliter-scale medical diagnostic devices; because of their economics, they also open up a pathway toward applications with much larger volumetric flow rates, while maintaining the inherent advantages of microfluidics. Take for example the large-scale liquid−liquid extraction processes commonly used in crude oil refinement, pharmaceutical production, and wastewater treatment.[12] The efficiency of extraction processes is often determined by the interfacial contact area between immiscible liquid phases (larger contact area is better), as well as the diffusion of solute from the bulk of each liquid to the liquid−liquid interface (faster diffusion and shorter diffusion paths being the goal). As stated above, the fundamental physical characteristics of microfluidic flow are very amenable to these requirements. Thus, faster, more efficient extractions with smaller reagent volumes could potentially be achieved if microfluidic devices can be produced sufficiently cheaply to be economically viable for processes with large volumetric flow rates.

The focus of this study is to investigate the feasibility of fabrics as large-scale microfluidic structures because existing textile manufacturing technologies offer proven economy-of-scale advantages. Fabrics are engineered porous structures that consist of yarns, which themselves are bundles of fibers or filaments. A woven fabric therefore contains two types of microscopic voids that can accommodate capillary flow: (1) the intra-yarn spaces between fibers or filaments within a yarn, and (2) the inter-yarn spaces between the yarns in a fabric. The textile manufacturing industry has developed scalable technologies to produce patterned fabrics that combine yarns of different types in repetitive geometrical structures with various degrees of complexity, ranging from simple plain weave structures to more complex architectures for specialty applications. Fluid flow within fabrics has been primarily studied, modified and exploited for use in so-called moisture management applications in which fluids are transported away from their source for storage or evaporation. Textile researchers have successfully explored surface coatings to modify the surface chemistry of fibers and yarns,[13−16] and it is well-known that variations in fabric construction parameters and material properties significantly affect fluid movement in fabrics.[17]

The premise of this paper is to extend the design of fabrics in a novel direction, aiming to control the fluid flow inside fabrics with precision and specificity akin to microfluidic devices. As mentioned above, the porous construction of a woven fabric naturally provides an intimately interconnected network of microchannels in the form of spaces within and between constituent yarns. By weaving hydrophobic and hydrophilic yarns together in a single fabric, we can thus create a network of microchannels with heterogeneous surface properties, which should allow for simultaneous flow of immiscible liquid phases with a large interfacial contact area. Standard textile production technologies provide a large design space with regards to fabric construction, and yarn properties (i.e., material, size, shape, surface chemistry). A wide variety of microfluidic channel designs can therefore be engineered and manufactured on industrial scales using existing facilities.

The main objectives of this study are to prove that: (1) careful design of woven amphiphilic fabrics yields a similar level of control over fluid motion as observed in microfluidic devices, and (2) coflow of immiscible liquid phases can be achieved with a large interfacial contact area, which makes the fabrics suitable as microcontactor substrates for liquid−liquid extraction processes, both on the laboratory scale and, because of scalable manufacturing technology, on industrially relevant scales.[18] In addition, potential single-fluid applications include cheap diagnostic microfluidic devices in which the flow paths of fluids are relatively simple in comparison with the very complex designs of some PDMS-based devices.

EXPERIMENTAL DESIGN

Capillary liquid flow in a porous medium is governed by the size, orientation and surface chemistry of the pores.[19,20] The wicking flow rate of liquid into a fabric is controlled predominantly by yarn placement, the spacing between yarns, and their surface chemistries. A distinguishing feature of this study is that we systematically investigated the effect of the placement of hydrophilic and hydrophobic yarns in amphiphilic fabrics to determine: (1) how effectively yarn placement can be used to control the flow path and flow rate of liquids into fabrics, and (2) if parallel flow of immiscible liquid phases can be achieved within an amphiphilic fabric. To systematically and unambiguously address these research questions, we limited the fabric architecture in our investigation to a plain weave, in which two sets of yarns ("weft" and "warp") intersect at right angles and in which each yarn alternately crosses over and under subsequent intersecting yarns. Furthermore, as will be described in detail below, we used two types of yarns with similar physical properties (diameter and fiber density), but different surface chemistries. Figure 1 depicts the weave patterns of five fabrics used in this study, with hydrophobic yarns shown in red (dark) and hydrophilic yarns in blue (light). Inspired by the standardized classification of surfactants in terms of hydrophilic/lipophilic balance, we developed a fabric nomenclature that captures the yarn pattern within a repeat unit in terms of the quantity and positional order of the two yarn types. Hydrophilic yarns are designated "H" and hydrophobic (or lipophilic) yarns "L". The fabric pattern is then specified by identifying a repeat unit for the fabric and listing the sequence of yarns within this repeat unit in both primary directions. For example, 2H-2L/4L (Figure 1b) describes a fabric in which pairs of like yarns

(2H and 2L) alternate in one direction, whereas only hydrophobic yarns (4L) are present in the other, perpendicular direction.

The fabric designs in Figure 1 highlight two structural features that were hypothesized a priori to affect fluid flow: "channels" and "intersections". A "channel" is defined as the void space between two parallel yarns. Because capillary flow relies on adhesive forces between the liquid and surrounding solid surfaces, capillary action is expected to be maximized when two yarns of the same surface chemistry are placed side by side; compare, for example, 1H-1L/4L in Figure 1a (no hydrophilic H−H channels) with 2H-2L/4L in Figure 1b (one hydrophilic H−H channel per repeat unit). Additionally, by using only one yarn type in a particular direction, the number of channels in that direction is maximized: fabric 4H/4L in Figure 1d possesses four vertical hydrophilic channels per repeat unit. It is important to reiterate that the term channel only refers to the inter-yarn void spaces, not to the intra-yarn voids between fibers within each yarn. As will be discussed in the Results section, capillary flow in intra-yarn void spaces does contribute to fluid flow. However, this first study of amphiphilic fabrics aimed to elucidate the effect of inter-yarn voids, which can be engineered via the weave pattern. Hence, all fabrics in this study were designed to have constant yarn diameters and intra-yarn spacing.

The second key structural feature of amphiphilic fabrics with regards to liquid flow are the so-called "intersections", perpendicular crossings of yarns (see, for example, 2H-2L/2H-2L in Figure 1c). Intersections of like yarns enable fluid transfer between orthogonal yarns and this connectivity creates alternative pathways for fluid flow between locations.

With the above definition of channels and intersections in mind, five different fabric samples were constructed, each with varying numbers of hydrophilic channels and intersections. For example, fabric 1L-1H/4L (Figure 1a) has no intersections and no channels between hydrophilic (H) yarns. Fabric 2H-2L/4L (Figure 1b), on the other hand, has one hydrophilic channel per repeat unit, but no intersections between hydrophilic yarns; sample 2H-2L/2H-2L (Figure 1c) has two hydrophilic channels and four intersections between hydrophilic yarns per repeat unit; sample 4H/4L (Figure 1d) has four hydrophilic channels per repeat unit, but no intersections. Finally, sample 4H/4H is the control fabric consisting of all hydrophilic yarns. By comparing fluid flow paths and rates in these five fabrics, we can systematically study contributions of these structural features of the fabrics to microscopic fluid flow.

Because of the potential applications of amphiphilic fabrics as lab-scale microfluidic devices for small liquid volumes and as industrial-scale continuously operated liquid−liquid microcontactors, the dynamics of liquid flow in these fabrics were evaluated for both scenarios. The water wicking rates and flow paths for the five fabric samples depicted in Figure 1 were analyzed via two methods: drop tests and upward wicking tests. In the drop tests, a single drop of liquid is placed on the fabric; liquid absorption and flow into the fabric then occurs from this finite liquid reservoir, analogous to microfluidic chips for medical diagnostic screenings. In this set-up, flow channels within the fabric compete for the finite volume of available liquid and the microscopic flow is thus expected to be time-dependent. In upward wicking tests, on the other hand, one end of a fabric strip is immersed in a large liquid reservoir, so that a continuous supply of liquid is available; this scenario more closely resembles continuous liquid−liquid extraction set-ups. Studying the flow

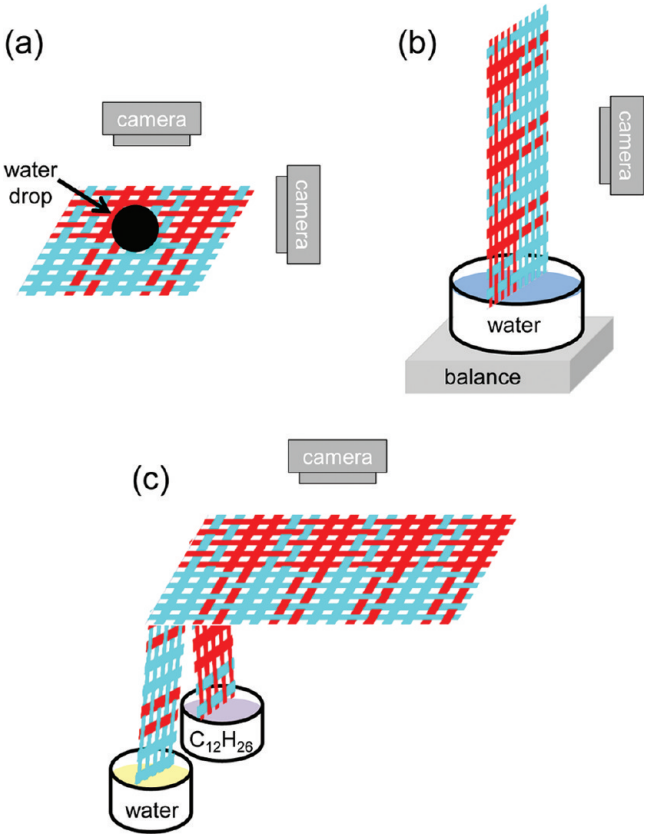

Figure 2. Experimental set-ups for monitoring fluid transport into fabrics: (a) drop test in which an overhead camera was used to capture flow path and a side-view camera was used to capture drop volume as a function of time, (b) upward wicking test from a reservoir in which a balance and camera were used, and (c) horizontal wicking test in which the end of a fabric strip was cut at the border between groups of parallel adjacent hydrophilic and hydrophobic yarns so that feeder strips could supply water and dodecane from two separate reservoirs.

dynamics for finite and infinite reservoirs will provide insight into behavior that is relevant for both applications.

The final experiment described in this paper is a two-phase horizontal wicking test with two immiscible fluids. This experiment was critical to determine if the insights from tests with a single fluid can be related to simultaneous flow of immiscible liquids, which is required for achieving liquid−liquid extractions in amphiphilic fabrics.

EXPERIMENTAL DETAILS

Materials. Commercially available fibers were obtained and ring spun into yarns by Patrick Yarns (Kings Mountain, NC). Delcron Hydrotec (DAK America) fibers (hydrophilic copolyester, 1.5 in length, 1.5 denier or 1.67×10^{-4} g/m) were spun to give white hydrophilic yarns (24 cotton count or 220 denier or 2.4×10^{-2} g/m) that were 230 μm in diameter with 146 fibers/cross section. Polypropylene fibers (1.4 denier or 1.56×10^{-4} g/m) from FiberVisions (Duluth, GA) were ring spun to give white hydrophobic yarns (26 cotton count or 202 denier or 2.2×10^{-2} g/m) that were 260 μm in diameter with 144 fibers/cross section. Twist levels (typically 12 to 18 turns/inch) were kept as low as possible to maximize fluid flow yet allow sufficient cohesion for spinning and weaving. The yarns were woven at the Textile Technology Center of Gaston College (Belmont, NC) on a computer-controlled dobby rapier

sample loom (SL7900, CCI Tech; New Taipei City, Taiwan) to give a plain weave fabric (20 × 72 in), with 75 yarns/inch in both warp and weft directions, resulting in a cover factor of 90%. The yarns were arranged in the warp and the weft was inserted to give a large variety of systematically different patterns of hydrophilic and hydrophobic yarns. Black tag yarns were then inserted to mark borders between different weave patterns. The creation of homogeneous fabrics with well-controlled yarn density is critical for the reproducibility of the experiments reported in this paper.

Water was deionized using a Millipore Direct-Q 5 ultrapure system. Anhydrous *n*-dodecane was used as purchased from Sigma Aldrich (purity >99%). Liquid food dyes used to color the water were McCormick (black) and Walmart Great Value (orange), which were both purchased locally. The dye used to color the dodecane was powdered Dispersol Blue 4PA (ICI Americas; Charlotte, NC).

Methods. *Drop Tests.* In the drop tests (cf. Figure 2a), a small rectangular fabric sample (15 mm ×8 mm) was placed on a microscope slide and secured at each end using self-adhesive tape. A 5 μL drop of water was then placed on hydrophilic yarns near the center of the fabric sample using an Eppendorf 20 μL pipet. Dyed water (black) was used to increase the contrast between wetted and dried fabric for image analysis purposes, but control studies with nondyed water were carried out to ensure that the dye did not affect the water wicking properties. Drop tests were recorded from the top to visualize fluid flow paths and from the side to quantitatively monitor drop volume evolution. Video microscopy was performed using Lumenera (Ottawa, Ontario) LU135 M monochrome and LU135C color cameras (for side and overhead views, respectively) in combination with a Leica Z6 APO zoom lens (Leica Microsystems; Buffalo Grove, IL), and Lucam Recorder image acquisition software (Astrofactum; Munich, Germany). The recorded images were analyzed with IDL (Interactive Data Language) image analysis software (ITT Visual Information Solutions; Boulder, CO), to determine the size of the diminishing water drop as a function of time. The volume of the liquid drop was calculated from the length of its base and its height, assuming that the drop had a spherical shape at all times; this assumption is reasonable because of the high surface tension of water and the small drop volumes in all tests.

Upward Wicking Tests. For upward wicking tests (cf. Figure 2b), 20 mm × 40 mm strips of fabric were used. The samples were hung vertically from a holding bridge constructed from FisherTechnik blocks (Studica, Inc.; Sanborn, NY). In front of this holding bridge was a camera to record the vertical progression of the wetting front of water as it was being absorbed into the fabric sample. A water reservoir (with black dyed water) was placed on top of a balance so that the mass of liquid absorbed into the fabric could be recorded; both the water reservoir and the balance were placed on top of a lab jack, which was raised until the fabric was submerged to a ∼1 cm depth at the start of each experiment. To minimize effects of air flow on balance measurements and to minimize variations in temperature and humidity, the experiments were conducted under a transparent Plexiglas cover. Analogous to the drop tests, a camera (Sony XC-ES50 with a Navitar 7000 Zoom Lens) was used to record the vertical progression of the wetting front into the fabric. The mass of liquid absorbed into the fabric was recorded via Labtronics Balance Talk XL data acquisition software (Labtronics Inc.; Guelph, Ontario) on a computer connected to the analytical balance (Sartorius Acculab VIC, Data Weighing Systems, Inc.; Elk Grove IL) via an RS232 serial port. Wicking data from the first 30 s of the test (ca. 1 cm of upward wicking distance) were fit with a straight line to determine the initial upward wicking rate. At times greater than 30 s, the slowing effects of gravity became apparent in the data.

Horizontal Two-Phase Wicking Tests. Horizontal two-phase wicking tests (cf. Figure 2c) were conducted on a 50 mm × 10 mm fabric sample of construction 5H-5L/2H-2L (also see Figure 6a). One end of the sample was placed on a microscope slide and secured to the slide using self-adhesive tape, creating a horizontal test section of ca. 15 mm. The rest of the fabric (∼35 mm) was draped over the edge of the slide and cut lengthwise along the border between hydrophilic and hydrophobic yarns to create feeder strips that could be immersed into separate reservoirs for water and dodecane. Liquid flow was initiated by filling the reservoirs with the appropriate liquids. To distinguish between the two naturally clear liquids, water was dyed orange and dodecane was dyed purple. Overhead images of the wicking process were again recorded using a Lumenera LU135C color camera with Leica Z6 APO zoom lens to resolve the two liquid streams.

RESULTS AND DISCUSSION

Drop Tests. Overhead drop tests revealed that flow paths and flow rates of water wicking into the amphiphilic fabrics can be controlled by the arrangement of hydrophilic and hydrophobic yarns. Figure 3 presents a comprehensive overview of the results of the drop tests for all five fabric samples: the top row of images (Figure 3a) is a schematic representation of the construction of each fabric, which is confirmed by the second row of UV-illuminated images (Figure 3b), in which the hydrophilic yarns appear bright because the polyester of which they are composed exhibits fluorescence; rows 3−6 (Figure 3c) present overhead views of the progression of fluid flow into the fabrics; finally, the bottom row is a side-view snapshot of the water drops 50 s after being placed on the fabrics. In addition, the results from the quantitative drop volume analysis for individual droplet experiments are shown in Figure 4.

As expected, the control fabric, 4H/4H, which contains no hydrophobic yarns that hinder the movement of water, exhibits very fast water flow in all directions and in all yarns. The drop absorption rate of 4H/4H is 2 orders of magnitude larger than any other fabric sample in this study, as indicated by the absence of a drop in Figure 3c after 50 s and the data in Figure 4. This control fabric represents the mechanism of liquid absorption into fabrics that one encounters in everyday life in most ordinary fabrics. However, when comparing water flow in 4H/4H with the other fabric samples, it becomes clear immediately that addition of hydrophobic yarns and variations in fabric design (i.e., placement of yarns) significantly alters the liquid flow rate and the flow path.

In sample 1H-1L/4L, water flows anisotropically, only along the hydrophilic yarn on which the drop was initially placed. Similar behavior is observed for sample 2H-2L/4L, albeit with a wider fluid channel formed by the adjacent hydrophilic yarns. In both cases, water only flows anisotropically because there are no hydrophilic intersections that facilitate liquid transfer in the perpendicular direction. Another important observation when comparing these two samples is the difference in the water absorption rates between 2H-2L/4L and 1H-1L/4L. The placement of the hydrophilic yarns in 2H-2L/4L creates a hydrophilic channel, which enables water flow between the hydrophilic yarns as well as within the yarns. As a result, more water can absorb in sample 2H-2L/4L than in 1H-1L/4L, as indicated by the darker color of the wetted strip in the images, at a higher rate. Figure 4 shows that the rate of water drop volume reduction is ∼80% greater in sample 2H-2L/4L than in 1H-1L/4L.

Looking at the data for 2H-2L/2H-2L in Figure 3, we see again that water initially flows only along the hydrophilic yarns on which the drop was placed. However, once the water encounters intersections with perpendicularly oriented hydrophilic yarns, it can reach yarns that were not wetted by the initial drop placement by following the network of intersecting yarns; this

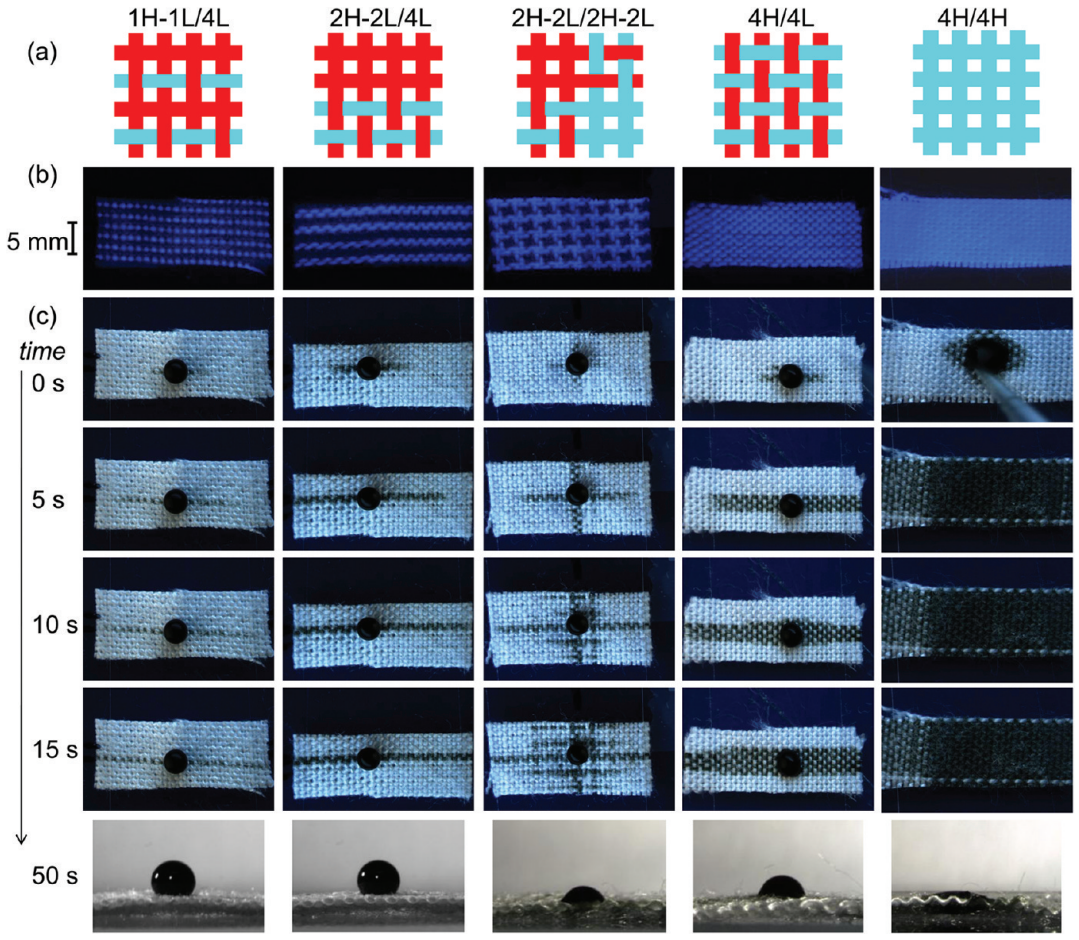

Figure 3. Single drops of water absorb into fabrics at rates and along paths governed by the arrangement and density of hydrophilic yarns: (a) fabric schematics, (b) UV-illuminated images in which hydrophilic polyester yarns are bright, and (c) time-resolved images of drop absorption. Each column represents a single fabric sample. Bottom row shows side view images of the water drop after 50 s.

flow pattern was not observed in samples 1H-1L/4L and 2H-2L/4L. Eventually, following the available fluid paths, water spreads throughout 2H-2L/2H-2L in a checkerboard fashion until the pattern of wetted channels mimics the fabric construction of the sample. Figure 4 shows that the presence of intersections in the fabric speeds up water absorption into the fabric; comparing the rate of absorption in 2H-2L/2H-2L with 2H-2L/4L, we notice a substantial increase by over 4 times.

Finally, analysis of the sample 4H/4L shows highly anisotropic wicking with preferential flow along the direction of the hydrophilic yarns. However, in contrast to 1H-1L/4L and 2H-2L/4L, water is able to slowly spread laterally to neighboring hydrophilic yarns that are outside the initial drop contact area, perpendicular to the H yarn orientation. The spreading occurs when the yarns are filled sufficiently with water to allow flow across channels to neighboring yarns. It is noteworthy that the lateral spread of water is much faster in 2H-2L/2H-2L (and 4H/4H), which provide hydrophilic intersections and therefore orthogonal H yarns, while 4H-4L offers merely channels that must be filled and crossed. Figure 4 shows that the high channel density of 4H/4L results in a drop volume reduction rate that is ~30% larger than for 2H-2L/2H-2L, making sample 4H/4L the amphiphilic sample with the fastest drop absorption rate. Although intersections are clearly helpful for spreading the liquid across the fabric samples, the larger hydrophilic channel density and larger initial contact area between the drop and hydrophilic yarns in 4H/4L dominate the initial water absorption rate presented in Figures 4b and c. It should be noted, however, that toward the end of the drop tests, when the finite size of the fabric samples becomes relevant, the absorption rate in 4H/4L slows down significantly as compared to sample 2H-2L/2H-2L, in which intersections offer alternative flow paths to the fluid. This is clearly shown in the bottom row of Figure 3c, where it is obvious that after 50 s the remaining drop on sample 4H/4L is larger than the drop on 2H-2L/2H-2L, despite the larger initial absorption rate. In conclusion, to increase the initial absorption rate of water, the addition of channels is more effective than the addition of intersections. Intersections, on the other hand, will facilitate spreading of the liquid throughout the entire fabric, thus increasing its absorptive capacity.

Upward Wicking Tests. The results from the upward wicking tests largely support the observations from the drop tests. Figure 5c displays the initial upward wicking rates for each fabric sample, which were determined from a linear least-squares fit to the mass versus time data recorded during the first 30 s of each test. Figure 5b shows images for each fabric sample 100 s after immersion into the dyed water.

Once again, the control fabric 4H/4H without hydrophobic yarns has by far the fastest upward wicking rate, over 5 times faster than any of the amphiphilic samples. Without hydrophobic

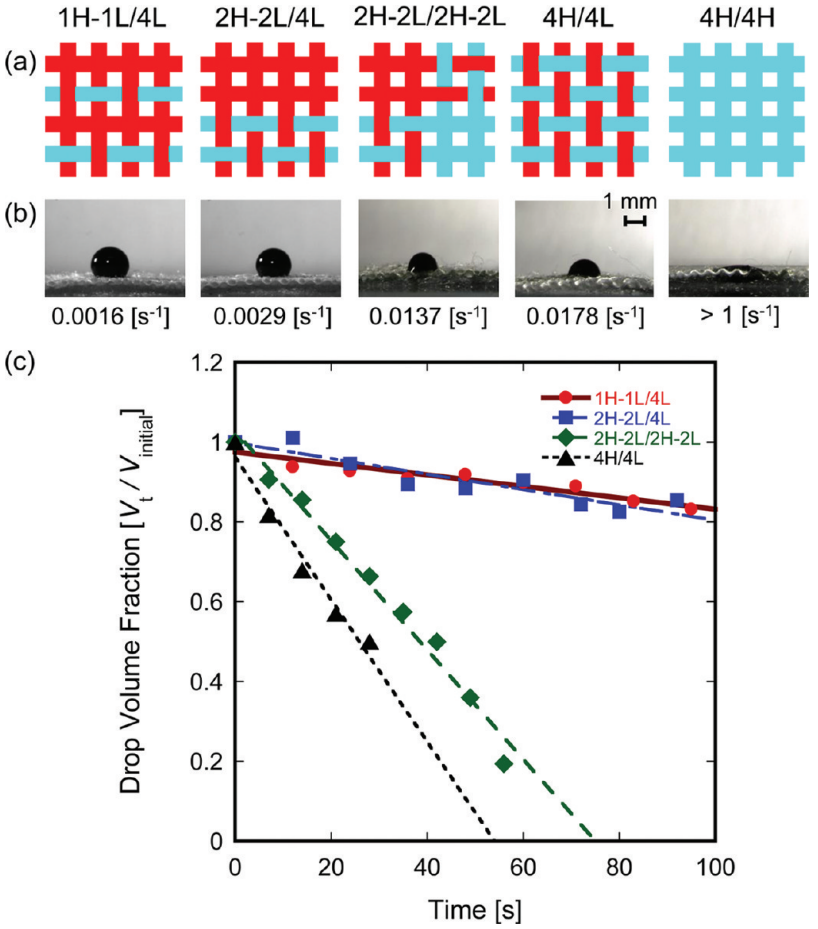

Figure 4. Quantitative analysis of water drop volume reduction versus time: (a) fabric schematics, (b) side view images of water drops 35 s after placement on fabrics; numbers below images are rates of drop volume reduction determined from (c) drop volume, normalized to initial volume, versus time for ●, 1H-1L/4L; ■, 2H-2L/4L; ♦, 2H-2L/2H-2L; and ▲, 4H/4L; lines are linear least-squares fits and slopes are rates of drop volume reduction listed in b. For the fully hydrophilic 4H/4H fabric, the drop was completely absorbed within 1 s.

yarns hindering the flow of the liquid, water can fully saturate the fabric, as indicated by the sharp wetting front in 4H/4H.

On the other end of the spectrum, in sample 1H-1L/4L, water only flows up into the hydrophilic yarns, which constitute every other vertical yarn, resulting in the slowest wicking rate. For sample 2H-2L/4L, the fraction of hydrophilic yarns in the vertical direction is the same, 50%, but the difference is that these yarns come in pairs, rather than as isolated yarns. The presence of hydrophilic channels in 2H-2L/4L has a significant effect on the wicking rate, which is 50% larger than for 1H-1L/4L, similar to drop test results presented in panels b and c in Figure 4.

The most complex fabric architecture, sample 2H-2L/2H-2L, exhibits interesting behavior in the upward wicking test. At the wetting front, water only flows vertically along pairs of hydrophilic yarns in that direction (cf. Figure 5b). However, behind the wetting front, water spreads in the transverse direction by transferring to orthogonal hydrophilic yarns at the intersections. This effect does not occur in samples 1H-1L/4L and 2H-2L/4L because there are no orthogonal H yarns, similar to the observation in the drop test. As shown in Figure 5c, hydrophilic intersections in the fabric allow water to wick into the fabric at a faster rate (~30%) than for sample 2H-2L/4L.

From the bar graph in Figure 5c, it can be seen that sample 4H/4L displays the fastest wicking rate among the amphiphilic fabrics, even 2 times faster than sample 2H-2L/2H-2L. The large number of hydrophilic channels in 4H/4L dominates the vertical wicking behavior. In these upward tests, where wicking occurs from an infinite reservoir, the need for lateral fluid spreading is not as critical as it was in drop tests on a finite fabric sample. In spite of the absence of intersections, liquid is still able to spread along the entire 4H/4L fabric length, because each hydrophilic yarn is in direct contact with the liquid reservoir. Hence, for upward wicking, the addition of channels has a larger effect on the wicking rate than the addition of intersections.

Figures 3−5 demonstrate unequivocally that weaving hydrophobic and hydrophilic yarns together into the same amphiphilic fabric allows for control over the flow path and rate of liquid absorption into the fabrics by engineering the fabric structure. The effects of changes in fabric structure on liquid flow path and flow rate were nominally the same for the drop tests and upward wicking tests, although the role of intersections is less important in the upward wicking tests. In conclusion, liquid flow can be controlled for both small drop volumes that are representative of microfluidic applications, and for wicking from reservoirs, which is more representative of large-scale industrial applications; there should not be significant differences between liquid flow dynamics upon scale-up of the fabric.

Parallel Flow of Immiscible Phases: Horizontal Two-Phase Wicking Tests. After concluding the single fluid experiments presented above, the next challenge was to test the second

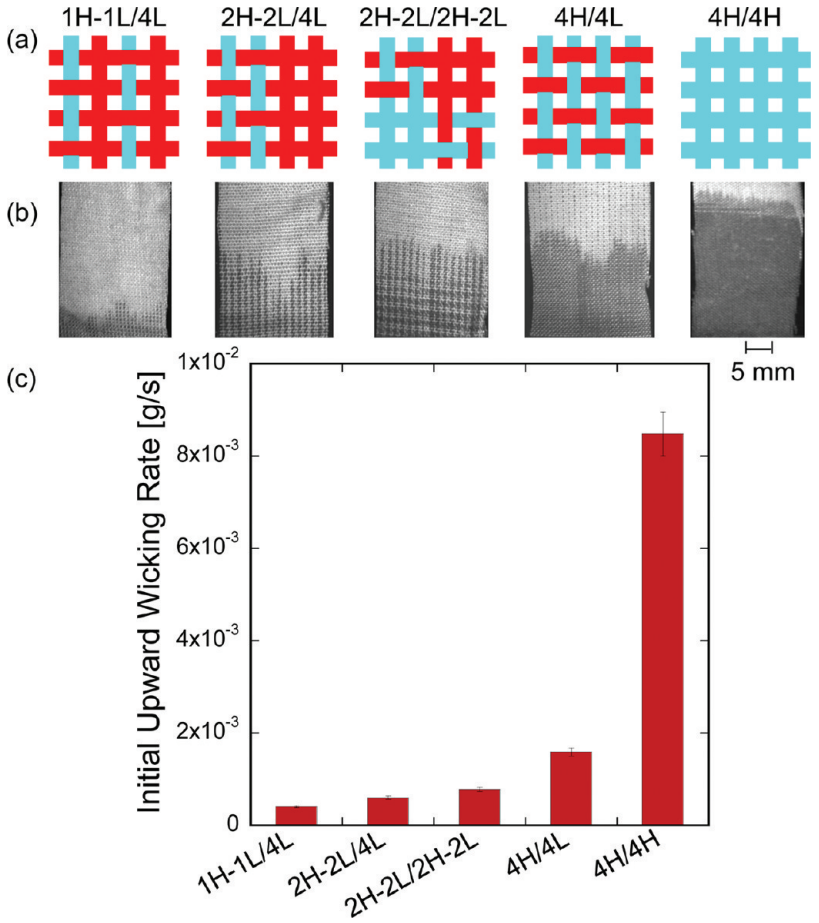

Figure 5. Upward wicking of water: (a) fabric schematics, (b) images showing flow patterns and wetting fronts after 100 s, and (c) initial upward wicking rates determined from linear least-squares fit to first 30 s of mass versus time data.

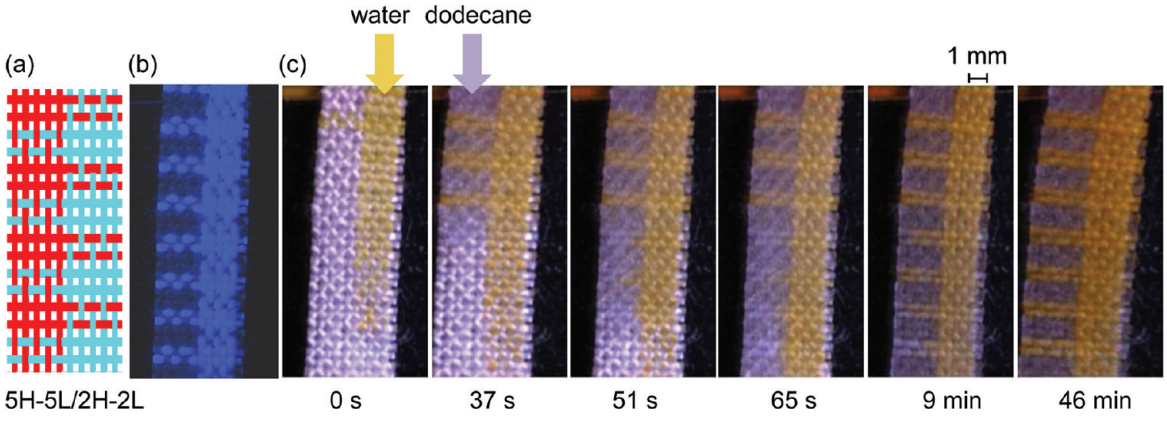

Figure 6. Co-flow of aqueous and hydrocarbon fluid in amphiphilic fabric 5H-5L/2H-2L: (a) fabric schematic, (b) UV-illuminated image of fabric that shows hydrophilic microchannels as bright regions, and (c) time-resolved overhead images that show water (stains yellow) wicks along the hydrophilic microchannels (prewicked into fabric already at $t = 0$) and dodecane (stains faint purple), which initially appears from the top left of image at 37 s as a darkening of the yarns, wicks along the hydrophobic microchannels. By 65 s, dodecane has wet the entire fabric not already wet by water, including perhaps some hydrophilic microchannels. By 46 min, water has filled all hydrophilic microchannels and the image exactly resembles the UV-illuminated image of the dry fabric shown in b.

hypothesis behind this study, namely that amphiphilic fabrics should enable simultaneous coflow of immiscible fluids. As described in the Methods section and illustrated in Figure 2c, a fabric strip was split into feeder strips that were immersed in water and dodecane, respectively. The series of images in Figure 6c display the wicking of water and dodecane into the horizontal section of the fabric, which had construction parameters 5H-5L/2H-2L. This fabric design was chosen because of the presence of channels and intersections for both yarn types. The larger groupings of 5 yarns in the primary flow direction

(as compared to pairs in 2H-2L/2H-2L) were selected to facilitate visual observation of the liquid phases. When water (dyed orange) wets the fabric, it stains the white hydrophilic yarns yellow; as dodecane (dyed purple) wets the fabric, it stains the white hydrophobic yarns a faint purple. In the two-phase wicking test, water was allowed to start wicking before dodecane to compensate for its slower wicking rate and allow both liquids to simultaneously enter the fabric area within the camera field-of-view. As a result, the first picture in Figure 6c, at time zero, only shows water in the fabric, no dodecane. In the subsequent images, it can clearly be seen that water and dodecane flow in parallel, filling their respective yarns. After 65 s, both water and dodecane have reached the end of the viewing area.

All hydrophilic yarns in the wicking direction are wetted with water. Dodecane has wetted all of the hydrophobic yarns in the wicking direction and the perpendicular direction; it even seems to have wetted the hydrophilic yarns that were not wetted by water yet, as indicated by the purple color.

Although dodecane was able to initially wet both hydrophilic and hydrophobic yarns, it does not prevent water from ultimately moving into the hydrophilic yarns, displacing the dodecane. The image after 9 min clearly shows that all transverse hydrophilic yarns are turning yellow and filling with water. The final image, taken after 46 min, shows that the coflow of the two immiscible liquids is stable: neither liquid phase was able to displace the other. The intimate interfacial contact between phases was maintained throughout the wicking experiment, which is very promising for liquid−liquid extraction experiments. In existing liquid−liquid extraction equipment, intense efforts (e.g., agitating phases via sieve trays, mixer paddles, rotating disks) must be made to create and sustain large interfacial contact areas between immiscible liquid phases that are necessary for efficient extractions.[18] In our amphiphilic fabrics, parallel flow of immiscible phases is simply facilitated by the surface chemistry of the yarns and microscopic capillary flow. These fabrics therefore show potential for performing highly efficient liquid−liquid extractions. This would be facilitated by the highly scalable nature of this technology, and by the large and widespread existing infrastructure for its production. Modern looms allow high speed production of fabrics with constructions that range from simple (e.g., plain weave) to enormously complex in terms of relative yarn arrangements and placement. Further studies (experimental and modeling) of the fluid flow of immiscible liquids in amphiphilic fabrics, both regarding flow patterns and flow rates, will be needed to fully exploit the capabilities of these novel substrates.

CONCLUSIONS

Wicking flow of aqueous fluids in micrometer-sized channels can be directed and controlled by precise placement of hydrophilic yarns into a woven fabric with hydrophobic yarns. The fluid is transported through voids between fibers that make up the yarns, and through microchannels between the yarns. Systematic variation in the numbers of adjacent parallel and orthogonal hydrophilic yarns allowed control of the areal density of inter-yarn microchannels that were hydrophilic, hydrophobic, and amphiphilic. Increasing density of inter-yarn hydrophilic microchannels significantly enhanced flow rates of aqueous fluids. The successful control of finite liquid volumes indicates that careful design of amphiphilic fabrics can be used to create simple microfluidic structures for various end-use applications. Amphiphilic microchannels were created by adjacent placement of hydrophilic and hydrophobic yarns. Simultaneous coflow of an aqueous and hydrocarbon fluid was demonstrated. This result, combined with the large interfacial contact area between immiscible fluids contained within an amphiphilic fabric, suggests these materials are potentially useful as large-area microcontactors for industrial-scale liquid−liquid extractions.

AUTHOR INFORMATION

Corresponding Author
*Email: victor.breedveld@chbe.gatech.edu.

ACKNOWLEDGMENT

Discussions on fabric and yarn construction with Krishna Parachuru of Georgia Tech are gratefully acknowledged. The hydrophobic fibers were provided by Jim Pepper of FiberVisions. We especially thank Gilbert Patrick of Patrick Yarns, for numerous discussions and critical guidance, for fiber sourcing, for yarn manufacturing, and for donating time and materials. Thanks also to Mitch Hensley of Patrick Yarns. John Anderson and John Fowler of the Textile Technology Center at Gaston College took the yarns and converted them into our amphiphilic fabrics. Support for this work was provided by the Department of Commerce through the National Textile Center.

REFERENCES

(1) Rivet, C.; Lee, H.; Hirsch, A.; Hamilton, S.; Lu, H. *Chem. Eng. Sci.* **2011**, *66*, 1490.
(2) Beebe, D. J.; Mensing, G. A.; Walker, G. M. *Annu. Rev. Biomed. Eng.* **2002**, *4*, 261.
(3) Hansen, C. L.; Skordalakes, E.; Berger, J. M.; Quake, S. R. *Proc. Natl. Acad. Sci. U.S.A.* **2002**, *99*, 16531.
(4) Balu, B.; Berry, A. D.; Hess, D. W.; Breedveld, V. *Lab Chip* **2009**, *9*, 3066.
(5) Lu, Y.; Shi, W. W.; Jiang, L.; Qin, J. H.; Lin, B. C. *Electrophoresis* **2009**, *30*, 1497.
(6) Martinez, A. W.; Phillips, S. T.; Butte, M. J.; Whitesides, G. M. *Angew. Chem., Int. Ed.* **2007**, *46*, 1318.
(7) Yager, P.; Kauffman, P.; Fu, E.; Lutz, B. *Lab Chip* **2010**, *10*, 2614.
(8) Fu, E.; Ramsey, S. A.; Kauffman, P.; Lutz, B.; Yager, P. *Microfluid. Nanofluid.* **2011**, *10*, 29.
(9) Reches, M.; Mirica, K. A.; Dasgupta, R.; Dickey, M. D.; Butte, M. J.; Whitesides, G. M. *ACS Appl. Mater. Interfaces* **2010**, *2*, 1722.
(10) Li, X.; Tian, J. F.; Shen, W. *ACS Appl. Mater. Interfaces* **2010**, *2*, 1.
(11) Ballerini, D. R.; Li, X.; Shen, W. *Biomicrofluidics* **2011**, *5*, 13.
(12) Green, D. W.; Perry, R. H. *Perry's Chemical Engineers' Handbook*; McGraw-Hill: New York, 2008.
(13) Coskuntuna, E.; Fowler, A. J.; Warner, S. B. *Text. Res. J.* **2007**, *77*, 256.
(14) Bajaj, P. *J. Appl. Polym. Sci.* **2002**, *83*, 631.
(15) Gupta, D.; Siddhan, P.; Banerjee, A. *Color. Technol.* **2007**, *123*, 248.
(16) Zhu, S. Q.; Hirt, D. E. *Text. Res. J.* **2009**, *79*, 534.
(17) Patnaik, A.; Rengasamy, R. S.; Kothari, V. K.; Ghosh, A. *Text. Prog.* **2006**, *38*, 105.
(18) Watson, J. S. *Separation Methods for Waste and Environmental Applications*; Marcel Dekker: New York, 1999.
(19) Bear, J. *Dynamics of Fluids In Porous Media*; Elsevier: New York, 1972.
(20) Dullien, F. A. L. *Porous Media Fluid Transport and Pore Structure*; 2nd ed.; Academic Press: San Diego, CA, 1979.